

Cell Surface Assembly of HIV gp41 Six-Helix Bundles for Facile, Quantitative Measurements of Hetero-oligomeric Interactions

Xuebo Hu,[†] Piyali Saha,[‡] Xiaoyue Chen,[†] Dogeun Kim,[†] Mahesh Devarasetty,[†] Raghavan Varadarajan,[‡] and Moonsoo M. Jin^{*†}

[†]Biomedical Engineering Department, Cornell University, Ithaca, New York, 14853, United States

[‡]Molecular Biophysics Unit, Indian Institute of Science, Bangalore, India 560012

S Supporting Information

ABSTRACT: Helix–helix interactions are fundamental to many biological signals and systems and are found in homo- or heteromultimerization of signaling molecules as well as in the process of virus entry into the host. In HIV, virus–host membrane fusion during infection is mediated by the formation of six-helix bundles (6HBs) from homotrimers of gp41, from which a number of synthetic peptides have been derived as antagonists of virus entry. Using a yeast surface two-hybrid (YS2H) system, a platform designed to detect protein–protein interactions occurring through a secretory pathway, we reconstituted 6HB complexes on the yeast surface, quantitatively measured the equilibrium and kinetic constants of soluble 6HB, and delineated the residues influencing homo-oligomeric and hetero-oligomeric coiled-coil interactions. Hence, we present YS2H as a platform for the facile characterization and design of antagonistic peptides for inhibition of HIV and many other enveloped viruses relying on membrane fusion for infection, as well as cellular signaling events triggered by hetero-oligomeric coiled coils.

Many proteins naturally fold into varying degrees of helix bundles, which are indispensable to normal physiology and to the onset of diseased states.¹ Well-known examples include viral membrane fusion proteins such as influenza virus hemagglutinin (HA) and HIV-1 envelope glycoprotein gp41. HIV infection critically depends on the attachment and fusion of the virus to host cells through the gp120/gp41 complex. The extracellular domain of gp41 consists of a fusion peptide, an N-terminal heptad repeat (NHR), a loop region, a C-terminal heptad repeat (CHR), and a membrane-proximal external region (MPER) (Figure 1a). Binding of gp120 to CD4 and subsequent interactions with coreceptors (CCR5 or CXCR4) lead to the dissociation of gp120 from gp41 and insertion of the viral gp41 fusion peptide into the target cell membrane, which then forms a prehairpin intermediate. Fusion of the viral and cellular membranes is provided by the formation of a gp41 six-helix bundle (6HB), a conformation described by three CHRs packed in an antiparallel manner on a central three-stranded NHR coiled coil^{2,3} (Figure 1b,c). The gp41 prehairpin intermediate is transiently accessible to viral fusion inhibitors derived from the NHR or CHR, which are called N and C peptides, respectively^{2,4–8} (Figure 1c,d). T20 is one of the early

C peptides developed for HIV fusion inhibition.^{9,10} CP32M, a rationally designed C peptide, extends to the upstream region of the CHR compared with T20 and contains mutations to enhance its affinity to the NHR. These result in higher thermostability and greater inhibition of viral infection against diverse HIV strains.¹¹ Compared with inhibitors derived from C peptides, there are fewer based on N peptides because of their low solubility. Five-helix (5H) peptides generated by linking in tandem 6HB peptides without their sixth C peptides have been used to mimic N peptides and shown to be highly stable and potent in viral inhibition.¹² Other N-peptide derivatives have been based on fusion to synthetic trimerization sequences.¹³ While much interest has been focused on developing synthetic inhibition peptides, natural peptides circulating in the blood have been reported to possess a capacity to inhibit virus fusion.¹⁴

The development of biochemical assays to examine the potency of inhibitors of 6HB formation has been hampered by the low solubilities of N and C peptides and their tendency to aggregate.¹⁵ As a facile and quantitative platform to study 6HB formation and to aid in the design of antagonistic peptides, we used the yeast surface two-hybrid (YS2H) system and expressed gp41 N and C peptides on the yeast cell surface. In YS2H, a system designed to express a pair of proteins for measuring protein–protein interactions,^{16,17} one protein is fused to yeast agglutinin and is thereby displayed on the yeast surface as the “bait”, while the other protein is secreted in soluble form and serves as the “prey” (Figure 2a,b). In the presence of an interaction, the two proteins associate with each other within the secretory pathway, and the prey is captured on the cell surface by the bait. The affinity of the interaction between the prey and the bait can be estimated quantitatively from the relative abundances of short tags fused to bait and prey, as typically measured by flow cytometry.¹⁷ This system has been used previously to study heterodimeric interactions; however, its applicability to studies of higher-order, complex oligomerizations has not been demonstrated.

To reconstitute the gp41 6HB complex on the yeast surface, we expressed N36 and C34,¹⁸ peptides derived from regions in the NHR and CHR, respectively (Figure 1d and Figure 2). N36 and C34 are known to form exclusively a 6HB complex devoid of any aggregates.^{3,18} Surface expression of N36 fused to Aga2

Received: February 2, 2012

Published: August 13, 2012

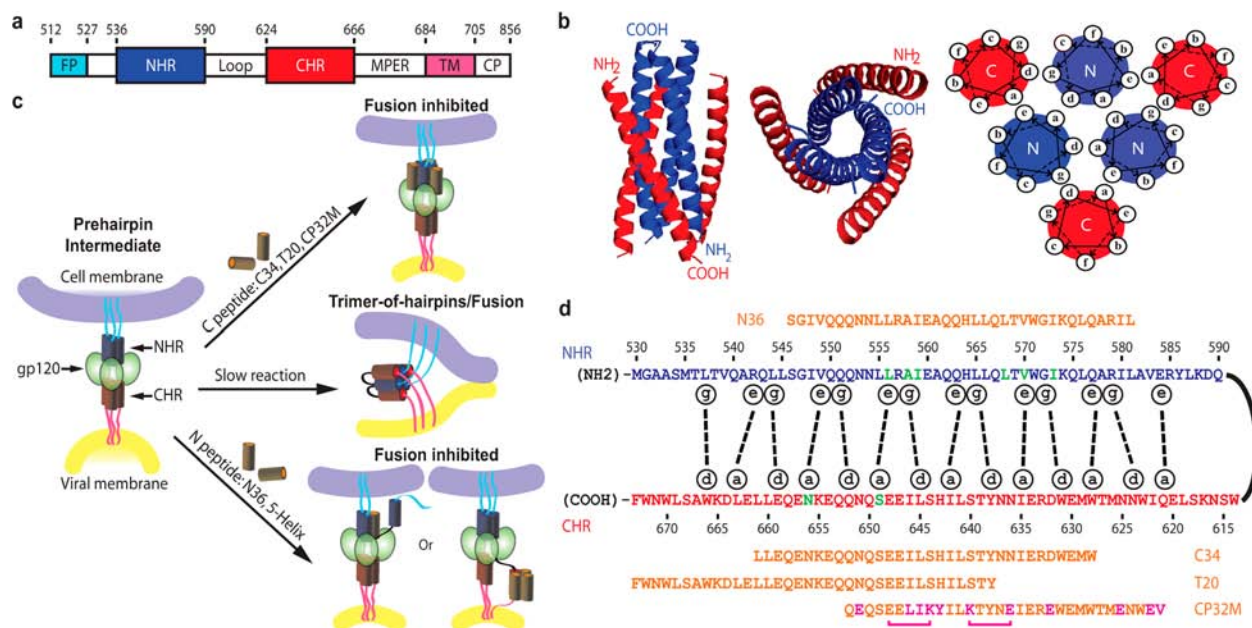


Figure 1. HIV-1 gp41 fusion complex driven by the formation of a trimer-of-hairpins composed of an NHR (blue) and a CHR (red). (a) Schematic view of gp41 elements. Residue numbers at the boundaries of each element are shown. (b) Ribbon drawings of side and top views of 6HB (PDB entry 1AIK³). The N- and C-termini of the helices are labeled. A helical wheel diagram is shown on the right, viewed from the C-terminal end of the NHR. (c) Events in HIV-1 membrane fusion and the mechanism of fusion inhibition by soluble N or C peptides. (d) Segments of the NHR and CHR of gp41. © through © denote the positions of heptad repeats in a helical wheel. Interacting pairs are delineated with dashed lines. The N and C peptides (orange) and single-point mutations (green) used in this study are indicated. CP32M contains rationally designed mutations (pink), some of which were made to introduce intramolecular salt bridges (pink square brackets). Abbreviations: FP, fusion peptide; NHR, N-terminal heptad repeat; CHR, C-terminal heptad repeat; MPER, membrane-proximal external region; TM, transmembrane domain; CP, cytoplasmic domain.

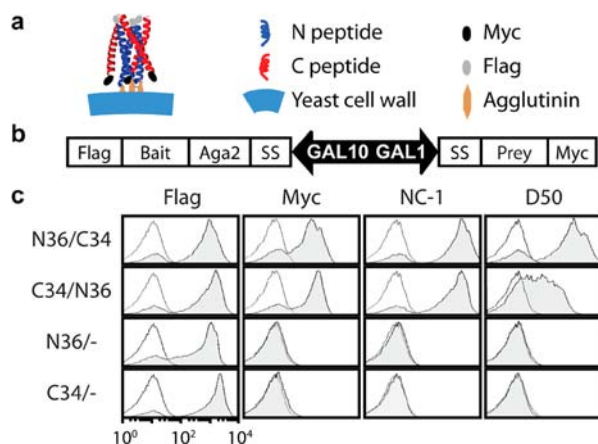


Figure 2. Assembly of 6HB on the yeast surface. (a) Schematic view of 6HB displayed on the yeast surface by YS2H. (b) In YS2H, the bidirectional promoter Gal1/Gal10 drives the expression of surface-anchored “bait” as a fusion to Aga2 and of secretory “prey”, the level of which is measured by antibody binding to the short epitope tags Flag and Myc, which are fused to the bait and the prey, respectively. “SS” denotes the signal sequence. (c) Immunofluorescence flow cytometry histograms of antibody binding to the Flag and Myc tags and gp41-specific antibodies (NC-1, D50). White- and gray-shaded curves are histograms of uninduced and induced yeast cells, respectively. “-” denotes no peptide.

(a subunit of agglutinin) as the bait was confirmed by antibody binding to a Flag tag appended to the C-terminus of N36. With C34 coexpressed as the prey, antibody binding to the Myc tag indicated capture of C34 by N36 (denoted as N36/C34 to refer to a pair of Aga2-fused bait and soluble prey; Figure 2b,c). N36/C34 association was further recognized by conformation-

specific monoclonal antibodies (mAbs) of gp41, NC-1¹⁹ and D50²⁰ (Figure 2c). Although the presumed epitope for D50 is at the C-terminus of the CHR (Ile642–Lys665),²⁰ yeast cells expressing C34 alone (C34/-) were not recognized by D50, indicating that C34 without N36 did not adopt a conformation existing in the context of 6HB. For C34/N36 (i.e., when N36 and C34 were swapped in the roles of bait and prey), similar levels of binding of tag-specific antibodies and the mAbs NC-1 and D50 were achieved (Figure 2c). We chose to anchor the N peptide as a fusion to Aga2 and secrete the C peptide as itself, a configuration more suitable for evaluating the potency of C-peptide-based antagonists.

To validate that in our YS2H system the N and C peptides were assembled into the conformation of 6HB previously seen in solution and crystals,^{3,18,21} we performed Western blots of N36/C34 peptides cleaved by TEV protease from the yeast surface (Figure 3). The staining pattern of the N36/C34 peptides by antibodies against the Flag and Myc tags closely matched that of the synthetic peptides (N36+C34) with identical amino acid sequences: one of the major bands from N36/C34 was identical to the ~40 kDa band from the synthetic peptides, which have been shown to reconstitute 6HB in solution.¹⁸ The identity of the ~40 kDa band to be 6HB was also corroborated by staining with the mAb NC-1. Compared with the synthetic peptides that formed one major band of 6HB, N36/C34 assembled in yeast did exhibit higher-molecular-weight bands stained by both antitag antibodies. We can speculate that during the secretory pathway, not all of the N36 and C34 peptides associate with each other to assemble into 6HB, with some N36 also forming higher-order oligomers that were still able to associate with C34 and retain NC-1 binding. In contrast to N36/C34 cleaved from yeast, N36

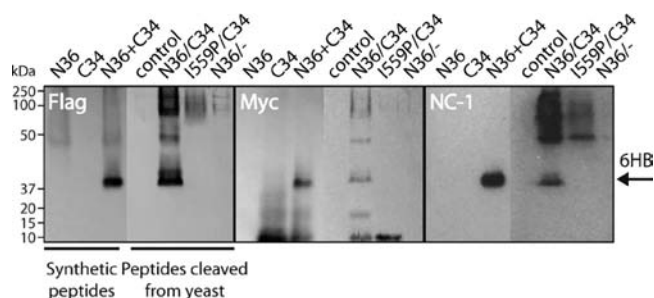


Figure 3. Confirmation of 6HB assembly in YS2H by Western blot. A TEV cleavage site was introduced immediately after the Flag tag following N36 and prior to Aga2 to permit enzymatic release of N36 from the yeast cell surface. Synthetic peptides containing amino acid sequences identical to those of cell-surface-cleaved N36/C34 were used as controls. N36/C34 before the induction of protein expression (control), N36 alone (N36/–), and N36 with the 6HB-disrupting mutation I559P (I559P/C34) were also included for comparison. Peptides were run on 12% native polyacrylamide gel. Molecular weight standards (Kaleidoscope Standards) were marked on the basis of their different colors.

alone (N36/–) and N36 with the 6HB-disrupting mutation I559P (I559P/C34; see below for details) did not produce a presumed 6HB complex band.

To examine whether YS2H would provide a quantitative readout of a change in hetero-oligomeric interactions, we introduced point mutations at various positions and measured the binding of antibodies against reporter tags and different oligomerization states of N36/C34 complexes (Figure 4). Physical forces contributing to 6HB or the coiled-coil conformation in general arise from the combination of van der Waals (vdW) or hydrophobic contacts at the helix–helix interface and electrostatic attraction among the residues positioned outside the interface. In a homotrimeric coil of NHRs, amino acids at the \oplus and \ominus positions in a helical wheel

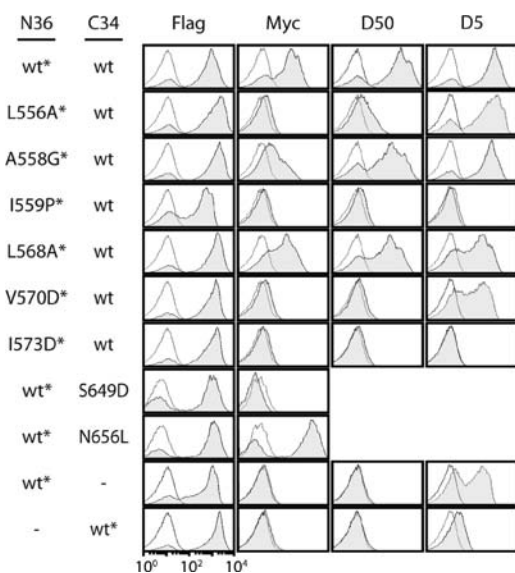


Figure 4. Immunofluorescence flow cytometry histograms of antibodies against Flag and Myc tags and antibodies (D50, D5) reactive to oligomeric forms of gp41. White- and gray-shaded curves are histograms of uninduced and induced yeast cells, respectively. “*” denotes Aga2-fused bait; “–” denotes no peptide; wt denotes wild type.

or heptad repeat form a helix–helix interface at the core (Figure 1b). The residues at the \oplus and \ominus positions of the NHRs would normally be those that promote electrostatic interactions, but here they are mainly hydrophobic to allow the CHR to pack onto the NHR homotrimer to form the 6HB. Mutations that disrupt hydrophobic or electrostatic forces would completely or partially disrupt the coiled-coil interactions. Mutations at the NHR–CHR interface (e.g., L556A at \oplus , A558G at \ominus , and V570D at \oplus of the NHR and S649D at \oplus of the CHR) led to modest (A558G) to almost complete (L556A, V570D, S649D) loss of C34 association with N36 (Figure 4). The SHB-specific mAb D5,²² which largely recognizes the hydrophobic pocket present at the C-terminal end of the NHR, displayed binding to 6HB mutants different from anti-Myc and D50. D5 showed strong binding to cells expressing only N36 (N36/–; Figure 4), revealing that without an assembly with C34, N36 adopts a conformation seen in the context of gp41. This is an important result that underscores the utility of yeast display, which circumvents the difficulty of studying isolated N-peptide derivatives in solution because of their hydrophobic, aggregation-prone nature. Mutations that disrupted a homotrimeric N-peptide conformation (e.g., I559P and I573D at \oplus of the NHR) therefore led to a complete loss of both anti-Myc and D5 antibodies (Figure 4). Such disruption of 6HB formation by I559P was also confirmed by Western blot (Figure 3). L568A, a mutation introduced at position \oplus of the NHR, least compromised the formation of 6HB. In contrast to various mutations that led to partial to complete perturbation of 6HB formation, N656L (at position \oplus of the CHR) led to an increase in the level of Myc expression (Figure 4), attributed to the introduction of a hydrophobic residue that would form vdW contacts with Ile548 and Val549 (Figure 1d).

After validating the assembly and perturbation of gp41 6HB, we examined the pairing of N36 or the full-length NHR (Met530–Gln590) with C34 variants such as T20 and CP32M, which have been developed as antagonistic C peptides for inhibiting HIV entry (Table S1 in the Supporting Information). The N36/T20 helix–helix interface is formed with three heptad repeats of the α -helix (Figure 1d), which is too short to produce a strong interaction, and this resulted in marginal binding of the anti-Myc antibody and D50. In contrast, NHR/T20, spanning longer than four heptad repeats of the α -helix at the interface, resulted in a level of Myc expression comparable to or less than the levels seen in NHR/C34 and N36/C34. The observation that NHR/T20 led to maximum binding with the mAb D50 is consistent with the fact that the D50 epitope is at the C-terminal end of the CHR (Ile642–Lys665), which is fully included in T20 but only partially present in C34.²⁰ When paired with either N36 or NHR, CP32M, a peptide spanning Gln621 to Gln652 of the CHR and containing mutations to enhance electrostatic and hydrophobic interactions with NHR, exhibited elevated levels of Myc expression. The lack of mAb D50 binding to N36/CP32M and NHR/CP32M occurs because the epitope of D50 is almost absent in CP32M. In YS2H, the levels of the reporter tags (Myc and Flag) are directly related by the Langmuir equation to the equilibrium dissociation constant (K_D) for the interaction between the bait and prey: $\text{Flag/Myc} = \alpha(1 + K_D/[prey])$, where α is the Flag/Myc ratio when $K_D \approx 0$. With the estimated values $\alpha = 4$ and $[prey] = 10$ nM in YS2H,¹⁷ values of K_D were obtained for binding of NHR or N34 to C34, T20, or CP32M (Table S1). Although direct measurements of the solution affinities for these pairs are not available, the differences in the affinities are

consistent with reported potencies of the C-peptide based inhibitors, which decrease in the order CP32M > C34 > T20.¹⁷ The ability to measure the equilibrium binding constants quantitatively highlights YS2H as a facile platform for predicting the potencies of antagonistic peptides.

In addition, YS2H can be adapted as a platform for measuring dissociation kinetics for hetero-oligomeric interactions. To minimize rebinding of dissociated C peptides to N peptides, yeast cells were washed and resuspended in a much larger volume of binding buffer (333-fold dilution of yeast culture), and antibody binding to the reporter tags was measured at different time points (Figure 5). Notably, the

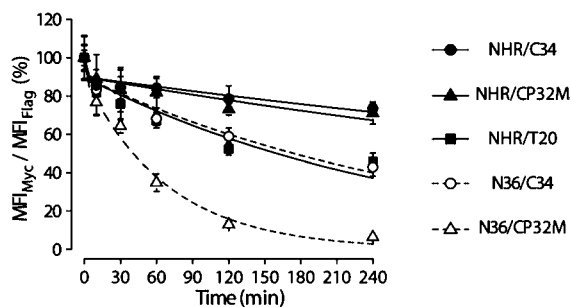


Figure 5. Dissociation kinetics of C-peptide inhibitors measured in YS2H. The loss of antibody binding to Myc (MFI_{Myc}) is plotted as a percentage after normalization to the level of antibody binding to Flag (MFI_{Flag}) ($n = 5$). A biphasic kinetic model was used to fit the data, and the fits are shown as solid or dotted lines.

decrease in antibody binding to Myc followed biphasic behavior characterized by a rapid reduction of Myc within the first 10 min followed by a slower decrease. An initial rapid dissociation of C peptide may be due to the loss of a small percentage (~15%) of C peptides that were associated with the N peptides to form nonideal 6HB complexes, some of which may correspond to higher-molecular-weight bands detected in the Western blot (Figure 3). When a biphasic dissociation model [$Y = A_1 \exp(-t/T_1) + A_2 \exp(-t/T_2)$] was used to fit the data, in agreement with the overall trend of dissociation, the slower kinetics were dominant ($A_1 \approx 15$ and $A_2 \approx 85$) for all interaction pairs measured (Table S1). Following a similar trend in the equilibrium affinities, the dissociation rate of C34 from NHR (NHR/C34; $16.2 \times 10^{-6} \text{ s}^{-1}$) was 3.5-fold slower than that from N36 (N36/C34; $56.7 \times 10^{-6} \text{ s}^{-1}$), and the dissociation rate of NHR/C34 was 3.9-fold slower than that of NHR/T20 ($62.7 \times 10^{-6} \text{ s}^{-1}$). Notably, although CP32M exhibited a higher equilibrium affinity to N36 than to C34 or T20, the dissociation rate of CP32M from N36 ($242.7 \times 10^{-6} \text{ s}^{-1}$) was 4.3-fold faster than that of C34 ($56.7 \times 10^{-6} \text{ s}^{-1}$) (Table S1), indicating that binding of CP32M to N36 is comparatively dominated by its on rate.

In summary, we have demonstrated the construction of a pair of α helices in the YS2H system and the assembly of the viral 6HB structure on the yeast cell surface. The equilibrium binding strengths of the coiled coils within the bundle as well as the kinetics of soluble peptides could be directly and quantitatively characterized. Subtle alterations resulting from single-point mutations perturbing the homotrimeric and hetero-oligomeric coiled coils could also be detected in YS2H, demonstrating its utility as a platform for the design, optimization, and evaluation of antagonistic peptides as drug candidates. Besides HIV, many enveloped viruses, including

influenza, respiratory syncytial virus, and Ebola virus, require helix bundles for membrane fusion during virus entry into the host.²³ In the past, a lot of effort has been directed toward the de novo synthesis of various types of helix bundles.^{24–28} The assembly of helix bundles or hetero-oligomeric peptides on the yeast surface would allow the rapid screening and design of candidate inhibitors without impediments from often unreliable in vitro protein refolding and costly chemical synthesis.

■ ASSOCIATED CONTENT

📄 Supporting Information

Materials and methods, Table S1, and complete refs 1–28. This material is available free of charge via the Internet at <http://pubs.acs.org>.

■ AUTHOR INFORMATION

Corresponding Author

mj227@cornell.edu

Notes

The authors declare no competing financial interest.

■ ACKNOWLEDGMENTS

The work was supported by NIH Grant GM090320, Northeast Biodefense Center U54-AI057158 (Lipkin) (to M.M.J.), and the Department of Biotechnology and Department of Science and Technology, Government of India (to R.V.). We thank the NIH AIDS Research and Reference Reagent Program, Division of AIDS, NIAID, NIH, for providing NC-1 and D50 antibodies and Dr. Joyce of Vaccines Basic Research, Merck Research Laboratories, for providing D5 IgG.

■ REFERENCES

- (1) Apostolovic, B.; et al. *Chem. Soc. Rev.* **2010**, *39*, 3541.
- (2) Weissenhorn, W.; et al. *Nature* **1997**, *387*, 426.
- (3) Chan, D. C.; et al. *Cell* **1997**, *89*, 263.
- (4) Chan, D. C.; et al. *Cell* **1998**, *93*, 681.
- (5) Jiang, S.; et al. *Nature* **1993**, *365*, 113.
- (6) Lu, M.; et al. *Nat. Struct. Biol.* **1995**, *2*, 1075.
- (7) Pan, C.; et al. *J. Formosan Med. Assoc.* **2010**, *109*, 94.
- (8) Root, M. J.; et al. *Proc. Natl. Acad. Sci. U.S.A.* **2003**, *100*, 5016.
- (9) Lalezari, J. P.; et al. *AIDS* **2003**, *17*, 691.
- (10) Greenberg, M. L.; et al. *J. Antimicrob. Chemother.* **2004**, *54*, 333.
- (11) He, Y.; et al. *Proc. Natl. Acad. Sci. U.S.A.* **2008**, *105*, 16332.
- (12) Root, M. J.; et al. *Science* **2001**, *291*, 884.
- (13) Bianchi, E.; et al. *Proc. Natl. Acad. Sci. U.S.A.* **2005**, *102*, 12903.
- (14) Munch, J.; et al. *Cell* **2007**, *129*, 263.
- (15) Gordon, L. M.; et al. *AIDS Res. Hum. Retroviruses* **1995**, *11*, 677.
- (16) Hu, X.; et al. *Proc. Natl. Acad. Sci. U.S.A.* **2010**, *107*, 6252.
- (17) Hu, X.; et al. *J. Biol. Chem.* **2009**, *284*, 16369.
- (18) Lu, M.; et al. *J. Biomol. Struct. Dyn.* **1997**, *15*, 465.
- (19) Jiang, S.; et al. *J. Virol.* **1998**, *72*, 10213.
- (20) Earl, P. L.; et al. *J. Virol.* **1997**, *71*, 2674.
- (21) Chan, D. C.; et al. *Proc. Natl. Acad. Sci. U.S.A.* **1998**, *95*, 15613.
- (22) Luftig, M. A.; et al. *Nat. Struct. Mol. Biol.* **2006**, *13*, 740.
- (23) Teissier, E.; et al. *Molecules* **2011**, *16*, 221.
- (24) Ulrich, L. E.; et al. *Bioinformatics* **2005**, *21* (Suppl. 3), iii45.
- (25) Dolphin, G. T. *J. Am. Chem. Soc.* **2006**, *128*, 7287.
- (26) Seo, E. S.; et al. *Biopolymers* **2007**, *88*, 774.
- (27) Rosenzweig, B. A.; et al. *Angew. Chem., Int. Ed.* **2009**, *48*, 2749.
- (28) Chakraborty, S.; et al. *Angew. Chem., Int. Ed.* **2011**, *50*, 2049.